

## Magnetic Measurement of the ELETTRA Storage Ring Prototype Magnets

F. Gnidica, S. de Panfilis, G. Petrucci\*, G. Stefanini\*, D. Tommasini, R.P. Walker and D. Zangrando, Sincrotrone Trieste, Padriciano 99, 34012 Trieste Italy and \*CERN, Geneva 23, CH 1211, Switzerland.

### Abstract

The results of magnetic measurements of the prototype gradient bending magnet, quadrupole and sextupole magnets for the ELETTRA storage ring are described.

### 1. INTRODUCTION

The 1.5-2 GeV ELETTRA storage ring [1] will contain 24 gradient bending magnets, 108 quadrupoles of three different lengths and 72 sextupoles of two different lengths. The design of the magnets was presented in ref. [2]. Prototypes of all three magnet types have been constructed by Ansaldo Componenti, Italy, and have been measured at CERN using the test systems set up for the ELETTRA magnets [3]. This report presents the results of these measurements, the comparison with design calculations, and discusses the changes that will be incorporated in the series production to further optimize the field quality.

The magnet measuring systems are now being re-commissioned at Trieste where they will be used to test the series magnets, the deliveries of which are due to commence in April this year.

### 2. DIPOLE PROTOTYPE

The main design parameters of the parallel-ended gradient bending magnet are summarized in Table 1. The magnet has been optimized for operation at 2 GeV, but with the capability of reaching a maximum of 2.4 GeV with lower field quality.

Table 1. Main dipole design parameters (2 GeV)

Bend angle	15°
Field	1.212 T
Field gradient	2.86 T/m
Field index	13
Bending radius	5.5 m
Steel length	1.370 m
Magnetic length	1.440 m
Gap (at beam position)	70 mm
Turns per pole	24

Measurements have been carried out using the automated three-axis measuring bench with a probe which consists of a linear array of 15 Hall plates with a 1 cm spacing [3]. Use of this probe allows a reduction in measurement time with respect to a single plate, together with improved accuracy. Errors introduced by uncertainties in the position of the individual plates are overcome by calculating the field after averaging the field gradient between successive points measured with different plates. Measurements were carried out in the median plane, both in the magnet centre to confirm the 2D pole profile, as well as field maps to confirm the 3D design calculations.

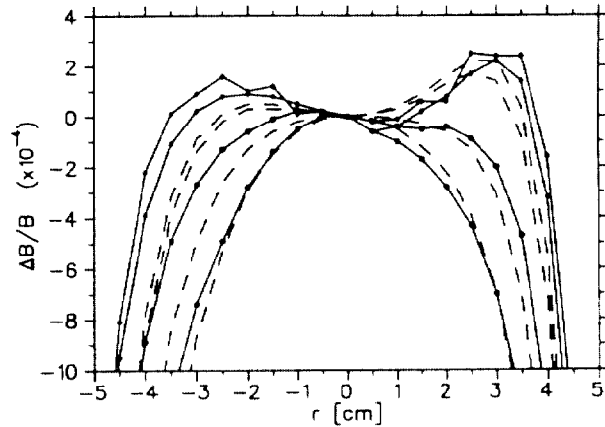


Fig. 1. Field uniformity in the centre of the dipole prototype at various current levels : in order, 700 A (upper curves), 1400 A, 1700 A and 1950 A (lower curves). Solid lines - measurements; dashed lines - calculations.

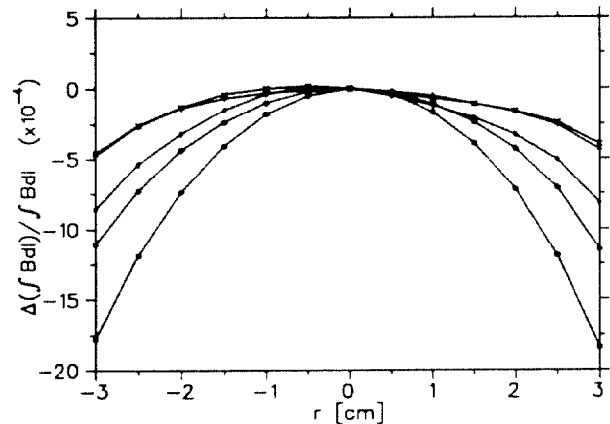


Fig. 2. Integrated field uniformity in the dipole prototype at various current levels : in order, 704 A (upper curve), 1055 A, 1427 A, 1618 A and 1950 A (lower curve).

Figure 1 shows the results of measurements in the magnet centre at various current levels. The field deviation with respect to values calculated with the measured central field and gradient (evaluated over the range  $\pm 2.5$  cm) is shown as a function of radial position,  $r$  positive signifying radially inwards. Between 700 A and 1400 A there is little change, followed by noticeable saturation. The measurements are in very good agreement with the expected performance, calculated with POISSON [4]. At 1.5 and 2 GeV the field homogeneity is within the specified limit of  $\pm 10^{-4}$  inside the defined good field region of  $\pm 2.5$  cm, and is within  $\pm 2.5 \cdot 10^{-4}$  at 2.4 GeV.

Table 2. Results of field maps of the dipole prototype.

I (A)	E (GeV)	$\rho_0$ (m)	$B_0$ (T)	$G_0$ (T/m)	$L_{\text{mag}}$ (m)	$\phi$ (deg.)	$S_0$ (T/m <sup>2</sup> )
703.6	1.00865	5.56795	0.60426	1.4174	1.4578	3.98	-0.28
1055.3	1.50628	5.55998	0.90367	2.1226	1.4556	3.67	-0.45
1427.1	1.99574	5.53313	1.20313	2.8169	1.4486	2.82	-1.11
1618.0	2.18510	5.50836	1.32321	3.0833	1.4420	2.12	-1.64
1950.0	2.43776	5.46771	1.48718	3.3868	1.4314	1.50	-2.98

Field maps were performed taking data at 10 different  $x$  positions and 44 different  $z$  positions up to  $z=1.3$  m, at which point the field had reduced to 0.03 % of its value at the magnet centre. Point spacing in  $z$  varied between 5 cm in the centre to 2 cm in the fringe field region. The analysis consisted firstly in finding the trajectory of the electron with appropriate energy ( $E$ ) which starts from the magnet centre and exits with the correct bending angle ( $\theta=7.5^\circ$ ). The field was then calculated along a series of curves parallel to the central trajectory, i.e. with constant perpendicular separation  $r$ , using a bi-cubic spline interpolation. The field integral variation, after subtracting the linear term, is shown in fig.2. The results were interpreted in terms of a hard-edge model in which the magnet has constant field  $B_0$ , gradient  $G_0$ , and sextupole term  $S_0$  with a magnetic length  $L_{\text{mag}}$ , and effective end-angle  $\phi$  (with respect to a sector magnet) :

$$\int B \, dl = (B_0 + G_0 r + S_0 r^2) (L_{\text{mag}} + (\tan \phi - \theta) r)$$

The field integral variation is well described by the above model; the residual error between the measured data and the fitted quadratic curve was always less than 0.01 %. The results of measurements at various current levels ( $I$ ) are summarized in Table 2.

The results show that the magnetic length, and hence also the bending radius at the magnet centre ( $\rho_0=L_{\text{mag}}/\theta$ ), are in very good agreement with the expected values. The central field is therefore close to the nominal value for a given energy. As regards the field gradient, the central field index ( $G_0\rho_0/B_0$ ) is 12.95 at 2 GeV, and hence very close to the desired value. The integrated gradient however is less than anticipated, the effective end angle being less than the nominal value of  $7.5^\circ$ . Alternatively, the data can be interpreted with a model in which the end-angle is defined to be  $7.5^\circ$ , but the effective field index is different from that at the magnet centre - 12.55 at 2 GeV. The physical reason for this behaviour is that the extent of the fringe field depends on the magnet gap, which decreases linearly with increasing radius,  $r$ . At high current levels saturation effects, which are greater at smaller values of the  $r$ , reduce the extent of the fringe field and hence further decrease the end-angle. The effect of the change in focussing strength of the magnet with respect to the nominal parameters has been investigated in [5]. Although the effects are small and acceptable, nevertheless the opportunity has been taken to modify the pole profile slightly in order to recover the nominal integrated gradient in the series magnets.

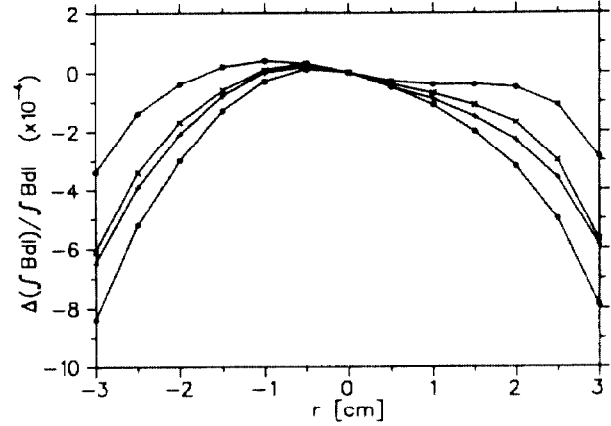


Fig. 3. Effect of various correction button geometries on the integrated field uniformity at an excitation of 1427 A (2 GeV). Lowest curve - no correction.

The sextupole field error, which according to fig.2 corresponds to a relative error of 0.05 % at  $r=\pm 2.5$  cm (2 GeV) would in principle also be acceptable compared to the limit set for the systematic sextupole component error of 0.08 % [6]. Nevertheless, experiments have shown that it is possible to reduce the error significantly by means of buttons placed on the end plate, as shown in fig. 3. In the best case studied so far the error reduces from 0.05 % to 0.015 % at  $r=\pm 2.5$  cm. Further tests will be carried out on the first series production magnet in order to define the optimum button geometry.

### 3. QUADRUPOLE PROTOTYPE

The quadrupole magnets are of a non-conventional 'open-sided' design, with upper and lower pole pairs not connected magnetically [2]. The three types required are identical in cross-section but have different lengths. The prototype quadrupole corresponds with the medium length type, with parameters given in Table 3. The short and long types will have steel lengths of 230 mm and 470 mm respectively.

Table 3. Main design parameters of the medium length quadrupole.

Inscribed radius	37.5 mm
Nominal gradient	20 T/m
Turns per pole	42
Steel length	380 mm
Nominal magnetic length	410 mm

A preliminary version of the quadrupole magnet was constructed in order to verify the pole profile, but not using the definitive method of assembly which will guarantee the correct pole placement. Measurements were carried out with the purpose built rotating coil system [3]. A coil with as large as possible outer radius (36.2 mm) was used in order to maximize sensitivity to the higher harmonics. The coil assembly includes a second coil with half the radius in order to distinguish between real harmonic field components (scaling as  $r^n$  for a 2n-pole field) and errors introduced by rotational inaccuracies (scaling as  $r$ ). In addition a rotating Hall plate was used in order to measure the field gradient in the centre of the magnet and hence determine the magnetic length. The radius (18.2 mm) was however too small to allow an accurate determination of the harmonic content as a function of longitudinal position. Further tests are planned using a probe with larger radius.

The measurements confirm that the required integrated strength is obtained at about 285 A, with magnetic length of 411 mm, in good agreement with 3D design calculations using TOSCA [7]. At this excitation level the reduction in integrated gradient due to steel saturation is 8.3 %. Table 4 presents the results of the measurements of the harmonic content; no significant variation with excitation level was observed.

Table 4. Harmonic content of the first prototype quadrupole at a reference radius of 25 mm, relative to the strength of the main component.

Component, n	Harmonic content (%)
3	0.075
4	0.033
5	0.008
6	0.050
14	0.005
other terms	< 0.001

Errors arising from the lack of symmetry (n=3,4,5) due to the provisional method of assembly are present as expected. The significant n=6 dodecapole error (negative in magnitude) arises from the fact that the magnet has a square end-profile. Measurements will be carried out to define an appropriate end-cut to remove the dodecapole error at a later stage.

#### 4. SEXTUPOLE PROTOTYPE

The sextupole magnets are of a similar open-sided design to that of the quadrupoles [2]. The prototype 'short' sextupole has main parameters given in Table 5. The 'long' version will have an identical cross-section, with 240 mm steel length.

Table 5. Main design parameters of the short sextupole magnet.

Inscribed radius	45 mm
Nominal field strength ( $B/r^2$ )	230 T/m <sup>2</sup>
Turns per pole	24
Steel length	125 mm
Nominal magnetic length	155 mm

Measurements were carried out using the same rotating coil system as above, both with a coil (outer radius = 43.7 mm) and with the Hall plate. The results confirmed that the required

integrated strength is obtained at 250 A, with somewhat shorter magnetic length (151 mm) than predicted by 3D design calculations using TOSCA [7]. At this level the reduction in strength due to saturation is 5.9 %. The measured harmonic content is given in Table 6; no appreciable variation was seen with magnet current.

Table 6. Harmonic content of the prototype sextupole at a reference radius of 25 mm, relative to the main component.

Component, n	Harmonic content (%)
4	0.105
5	0.040
6	0.037
7	0.006
9	0.025
other terms	< 0.001

The main error component is an octupole field arising from errors in the mechanical symmetry, however it is acceptable given the less stringent requirements for this magnet with respect to the quadrupole. Nevertheless, the series magnets will be assembled with an improved system for pole positioning that should lead to reduction in this value.

#### 5. ACKNOWLEDGEMENTS

The contributions of R.Grabit, A.Gubertini, P.Knobel and C.Rosset to the development of the measurement system, and in undertaking magnet alignment and measurement are gratefully acknowledged.

#### 6. REFERENCES

- [1] ELETTRA Conceptual Design Report, Sincrotrone Trieste, April 1989.
- [2] G.Petrucci et. al., Proc. 1990 EPAC, Nice, June 1990, p. 1119
- [3] G.Petrucci et. al., *ibid*, p. 1139
- [4] CERN-POISSON Program Package, F.Holsinger and C.Iselin
- [5] F.Iazzourene, Sincrotrone Trieste Internal Report ST/M-TN-92/2.
- [6] A.Wrulich, Sincrotrone Trieste Internal Report ST/M-TN-88/23.
- [7] TOSCA, Vector Fields, version 5.5